Journal of Zhejiang University-SCIENCE A (Applied Physics & Engineering)
ISSN 1673-565X (Print); ISSN 1862-1775 (Online)
www.jzus.zju.edu.cn; www.springerlink.com
E-mail: jzus@zju.edu.cn

A composite quadrature element with unequal order integration for consolidation problems*

Shuai YUAN[1], Hong-zhi ZHONG[†‡2]

[1]*Institute of Geotechnical Engineering, School of Highway, Chang'an University, Xi'an 710064, China*

[2]*Department of Civil Engineering, Tsinghua University, Beijing 100084, China*

[†]E-mail: hzz@tsinghua.edu.cn

Received Apr. 22, 2017; Revision accepted Oct. 30, 2017; Crosschecked June 6, 2018

Abstract: The weak form quadrature element method is a high-order algorithm which has been applied successfully to consolidation analysis of saturated and unsaturated soils. Its superiority over the conventional finite element method has been verified. However, in consolidation analysis, pore pressure oscillations will appear when small time increments are used due to the very small permeability and near-incompressibility of the pore water. This can produce almost zero values of main diagonal elements in the coefficient matrix. To overcome the pressure oscillations, we propose a coupled composite quadrature element in which different orders of integration are employed for the pore pressure and the displacement. Its performance is evaluated and compared with that of the standard element through 1D and 2D numerical tests. Our results show that pressure oscillations can be effectively alleviated and stability and accuracy can be significantly enhanced by using the proposed element.

Key words: Weak form quadrature element method; Unequal order integration; Numerical oscillations; Consolidation analysis
https://doi.org/10.1631/jzus.A1700218 **CLC number:** TU4

1 Introduction

The deformation of soils when loaded by external forces is time dependent. This has been studied broadly by scholars and engineers and many models have been proposed to describe the complicated behavior of soil consolidation. The theory put forward by Biot (1941) for 3D problems remains one of the most applied models for saturated soils in practice. Biot's model consists of continuity of pore fluid flow and differential equilibrium equations of soil taking into account the coupling of the dissipation of pore fluid pressure and the deformation of the soil skeleton. As for unsaturated soils, one of the most well-known models was proposed by Darkshanamurthy et al. (1984). Based on those models, a number of analytical and numerical solutions have been obtained (Samimi and Pak, 2012; Yuan and Zhong, 2014, 2016b; Azari et al., 2015; Ho and Fatahi, 2015; Ho et al., 2016).

Biot's model is frequently solved by the finite element method (FEM). Satisfactory results can be obtained when the approximated variable is smooth. However, if equal order interpolation is used for the displacement and the pore pressure, pore pressure oscillations will appear when small time increments are used due to the very small permeability and near-incompressibility of the pore water. This can produce almost zero values of the main diagonal elements in the coefficient matrix. Some stabilization procedures have been presented to allow for the use of equal order interpolation. Errors in the initial stage of consolidation were studied by Reed (1984) and a

‡ Corresponding author

* Project supported by the Natural Science Basic Research Plan in Shaanxi Province of China (No. 2018JQ5098) and the China Postdoctoral Science Foundation (No. 2017M613032)

ORCID: Shuai YUAN, https://orcid.org/0000-0002-8288-6858

© Zhejiang University and Springer-Verlag GmbH Germany, part of Springer Nature 2018

Gauss point smoothing technique was developed to smooth the initial pressure. A stabilized formulation was developed by Mira et al. (2003) through the introduction of an additional strain based on the enhanced strain element of Simo-Rifai (Simo and Rifai, 1990). Other stabilization approaches add a stability term into the continuity equation of Biot's model. The formulations derived by Aguilar et al. (2008), Rodrigo et al. (2016), and Preisig and Prévost (2011) fall into this group. Different stabilizations were reviewed and investigated by Preisig and Prévost (2011) and the effectiveness of those stabilizations was confirmed by 1D and 2D consolidation problems. The parameters of these procedures must be properly chosen otherwise the stabilizations fail to work.

An alternative is to use Taylor-Hood elements or composite elements with interpolation of the displacement one order higher than that of the pore pressure. Performance of different elements for consolidation was evaluated by Sandhu et al. (1977) who concluded that pressure oscillations produced by composite elements would disappear with the evolution of time if the Crank-Nicolson scheme is used for time integration, whereas those produced by standard elements would not. However, the accuracy of initial settlement obtained by composite elements is low compared with that obtained by standard elements.

The idea of composite elements has also been applied to other methods. Hua (2011) developed an element-free Galerkin (EFG) numerical model for consolidation in which the singularity of the system matrix was avoided by arranging fewer pressure points than displacement points. A radial interpolation meshless method with approximation of the displacement one order higher than that of the pore pressure was proposed by Wang et al. (2007) to overcome the spurious oscillations that occur when using the Crank-Nicholson time discretization scheme. Their method uses identical node distributions for the pore pressure and the displacement. Finite difference methods (FDMs) based on staggered grids have been established by Gaspar et al. (2003, 2006, 2016) and Boal et al. (2011) for 1D and 2D quasi-static consolidation, dynamic consolidation, and nonlinear consolidation, respectively. Using these methods, non-physical pressure oscillations can be removed completely by using different points for the displacement and the pore pressure.

The weak form quadrature element method (QEM) is a high order algorithm (Zhong and Yu, 2009) characterized by global approximation and rapid convergence. Numerical implementation of the quadrature element formulation is more straightforward because it requires less upfront data preparation. The integration points and the nodes are located at the same places and the post processing is very simple. The QEM has been applied successfully in seepage and consolidation analysis of soils (Yuan and Zhong, 2014, 2016a, 2016b, 2017).

The aim of the present study was to improve the stability of the QEM for consolidation analysis, especially in the initial stage of consolidation, by proposing a composite quadrature element. Unlike the standard quadrature element used in previous studies, in the composite element the integration of the displacement is taken as one order higher than that of the pore pressure to meet the necessary conditions for stability of consolidation problems. Consequently, different sampling points are employed for the pore pressure and the displacement. However, loss of accuracy of the pore pressure is negligible because of the characteristic of high order approximation. To our knowledge, research on high order composite elements has not previously been published. Numerical examples are given and the performance of the proposed element is compared with that of the standard element.

In this study, governing equations for consolidation are introduced first and the formulations of the composite quadrature element are derived in detail. Then, some key modifications are introduced about the QEM. At last, numerical tests are conducted.

2 Biot's model of consolidation

In this paper, boldfaced letters indicate matrices and vectors and boldfaced letters with subscripts i, j, l stand for their values at nodes (i, j, l). The pore pressure p, the stress $\boldsymbol{\sigma}$, and the strain $\boldsymbol{\varepsilon}$ are all positive for compression. The body force and the compressibility of pore fluid and solid grains are neglected for simplicity. The weak form description of Biot's theory is given as

$$\int_V \delta\boldsymbol{\varepsilon}^{\mathrm{T}}\boldsymbol{E}\boldsymbol{\varepsilon}\mathrm{d}V + \int_V \delta\boldsymbol{\varepsilon}^{\mathrm{T}}\boldsymbol{M}p\mathrm{d}V - \int_{S^t} \delta\boldsymbol{u}^{\mathrm{T}}\boldsymbol{T}\mathrm{d}S = \boldsymbol{0}, \quad (1)$$

$$\int_V (\nabla\delta p)^{\mathrm{T}} \frac{\boldsymbol{K}}{\gamma_{\mathrm{w}}} \nabla p\mathrm{d}V - \int_V \delta p\boldsymbol{M}^{\mathrm{T}}\dot{\boldsymbol{\varepsilon}}\mathrm{d}V + \int_{S^n} \delta p v_n \mathrm{d}S = 0, \quad (2)$$

where V and S denote the volume and the area of the domain, δ means the variation of variables, $\boldsymbol{E}$ is the elasticity matrix of the soil skeleton, $\boldsymbol{u}$ is the displacement vector, $\boldsymbol{T}$ is the prescribed surface force on boundary S^t, γ_{w} is the unit weight of the pore fluid, $\boldsymbol{K}$ is the permeability matrix, v_n is the prescribed normal filtration velocity on S^n, and the identity vector is $\boldsymbol{M}=[1\ 1\ 1\ 0\ 0\ 0]^{\mathrm{T}}$. Eq. (1) indicates the equilibrium of the soil skeleton and Eq. (2) the continuity of the pore fluid flow.

3 Formulations of the composite element

In the weak form quadrature element formulation, the solution domain is first discretized into subdomains (elements), and integrals in the weak form description of a problem in a given element are then evaluated by numerical integration. In the composite quadrature element, integrals corresponding to the displacement and the pore pressure are integrated individually using different integration points (Fig. 1). Integration of the displacement is one order higher than that of the pore pressure. Introduction of numerical integration into the equilibrium equation yields

$$\begin{aligned}&\sum_{i=1}^{N_\xi}\sum_{j=1}^{N_\eta}\sum_{k=1}^{N_\varsigma} W_i W_j W_k \delta\boldsymbol{\varepsilon}_{ijk}^{\mathrm{T}}\boldsymbol{E}_{ijk}\boldsymbol{\varepsilon}_{ijk}\left|\boldsymbol{J}\right|_{ijk}\\ &\quad+\sum_{i'=1}^{N'_\xi}\sum_{j'=1}^{N'_\eta}\sum_{k'=1}^{N'_\varsigma} W_{i'}W_{j'}W_{k'}\delta\boldsymbol{\varepsilon}_{i'j'k'}^{\mathrm{T}}\boldsymbol{M}p_{i'j'k'}\left|\boldsymbol{J}\right|_{i'j'k'}\\ &\quad-\sum_{k=1}^{N_S}\sum_{i=1}^{N_{k1}}\sum_{j=1}^{N_{k2}} W_i W_j \delta\boldsymbol{u}_{ij}^{\mathrm{T}}\boldsymbol{T}_{ij}\left|\bar{\boldsymbol{J}}\right|_{ij} = \boldsymbol{0},\end{aligned} \quad (3)$$

where W_i, W_j, and W_k are the weighting coefficients of the integration scheme, $|\boldsymbol{J}|$ is the Jacobian between the physical domain and the normalized domain, N_S is the number of prescribed surface forces, N_{k1} and N_{k2} are the numbers of integration points in the kth surface, $\left|\bar{\boldsymbol{J}}\right|$ is the Jacobian for the surface, N_ξ, N_η, and N_ς are the numbers of integration points for the displacement, and N_ξ', N_η', and N_ς' are the numbers of integration points for the pore pressure. The relation between the number of integration points for the displacement and that for the pore pressure is

$$N'_\xi = N_\xi - 1, \quad N'_\eta = N_\eta - 1, \quad N'_\varsigma = N_\varsigma - 1. \quad (4)$$

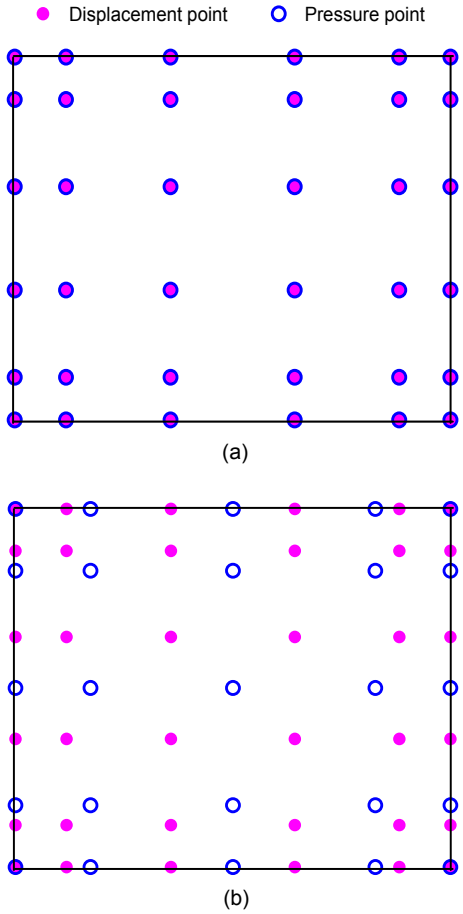


Fig. 1 Standard quadrature element (a) and composite quadrature element (b)

The Legendre-Gauss-Lobatto integration rule is adopted here. Denoting u, v, and w as the three components of the displacement vector, the strain can be expressed in terms of the nominal strain $\bar{\boldsymbol{\varepsilon}}$ in the normalized domain as Eq. (5), where x, y and z are the coordinates in the physical domain, and ξ, η, and ζ are the coordinates in the normalized domain, and $\boldsymbol{D}$ is a transformation matrix defined as Eq. (6).

$$\boldsymbol{\varepsilon}=\boldsymbol{D}\bar{\boldsymbol{\varepsilon}}, \tag{5a}$$

$$\boldsymbol{\varepsilon}=-\left[\frac{\partial u}{\partial x}\ \frac{\partial v}{\partial y}\ \frac{\partial w}{\partial z}\ \frac{\partial w}{\partial y}+\frac{\partial v}{\partial z}\ \frac{\partial w}{\partial x}+\frac{\partial u}{\partial z}\ \frac{\partial u}{\partial y}+\frac{\partial v}{\partial x}\right]^{\mathrm{T}}, \tag{5b}$$

$$\bar{\boldsymbol{\varepsilon}}=-\left[\frac{\partial u}{\partial \xi}\ \frac{\partial u}{\partial \eta}\ \frac{\partial u}{\partial \varsigma}\ \frac{\partial v}{\partial \xi}\ \frac{\partial v}{\partial \eta}\ \frac{\partial v}{\partial \varsigma}\ \frac{\partial w}{\partial \xi}\ \frac{\partial w}{\partial \eta}\ \frac{\partial w}{\partial \varsigma}\right]^{\mathrm{T}}, \tag{5c}$$

$$\boldsymbol{D}=\begin{bmatrix} J_{11}^{-1} & J_{12}^{-1} & J_{13}^{-1} & 0 & 0 & 0 & 0 & 0 & 0\\ 0 & 0 & 0 & J_{21}^{-1} & J_{22}^{-1} & J_{23}^{-1} & 0 & 0 & 0\\ 0 & 0 & 0 & 0 & 0 & 0 & J_{31}^{-1} & J_{32}^{-1} & J_{33}^{-1}\\ 0 & 0 & 0 & J_{31}^{-1} & J_{32}^{-1} & J_{33}^{-1} & J_{21}^{-1} & J_{22}^{-1} & J_{23}^{-1}\\ J_{31}^{-1} & J_{32}^{-1} & J_{33}^{-1} & 0 & 0 & 0 & J_{11}^{-1} & J_{12}^{-1} & J_{13}^{-1}\\ J_{21}^{-1} & J_{22}^{-1} & J_{23}^{-1} & J_{11}^{-1} & J_{12}^{-1} & J_{13}^{-1} & 0 & 0 & 0 \end{bmatrix}, \tag{6}$$

where J_{ij}^{-1} indicates the components of the inverse of the Jacobian matrix. Then the differential quadrature analogue is introduced and the strain at some integration point can be expressed in terms of the element displacement vector $\boldsymbol{d}^{\mathrm{e}}$ as

$$\begin{aligned}\boldsymbol{\varepsilon}_{ijk}&=\boldsymbol{D}_{ijk}\bar{\boldsymbol{\varepsilon}}_{ijk}\\ &=-\boldsymbol{D}_{ijk}\left[\sum_{m=1}^{N_\xi}C_{im}^{\xi}u_{mjk}\ \sum_{m=1}^{N_\eta}C_{jm}^{\eta}u_{imk}\ \sum_{m=1}^{N_\varsigma}C_{km}^{\varsigma}u_{ijm}\right.\\ &\quad\left.\sum_{m=1}^{N_\xi}C_{im}^{\xi}v_{mjk}\ \sum_{m=1}^{N_\eta}C_{jm}^{\eta}v_{imk}\ \sum_{m=1}^{N_\varsigma}C_{km}^{\varsigma}v_{ijm}\right.\\ &\quad\left.\sum_{m=1}^{N_\xi}C_{im}^{\xi}w_{mjk}\ \sum_{m=1}^{N_\eta}C_{jm}^{\eta}w_{imk}\ \sum_{m=1}^{N_\varsigma}C_{km}^{\varsigma}w_{ijm}\right]^{\mathrm{T}}\\ &=-\boldsymbol{B}_{ijk}\boldsymbol{d}^{\mathrm{e}},\end{aligned} \tag{7}$$

where $\boldsymbol{B}_{ijk}$ is the strain matrix in the QEM, and C_{im}^{ξ} is the weighting coefficient for the differential quadrature analogue. The essence of the differential quadrature analogue is the expression of a function derivative in terms of weighted linear summation of function values at all grid points. For details on the differential quadrature analogue, one may refer to (Bellman and Casti, 1971; Wang and Gu, 1997; Chen et al., 2005). Note that the strain $\boldsymbol{\varepsilon}_{i'j'k'}$ in the second term of Eq. (3) is defined on the pressure points, which should be expressed in terms of the displacements on displacement points. A strategy based on Lagrange interpolation is proposed. The strain on a pressure point is firstly interpolated by all the strains on displacement points:

$$\boldsymbol{\varepsilon}_{i'j'k'}=\sum_{i=1}^{N_\xi}\sum_{j=1}^{N_\eta}\sum_{k=1}^{N_\varsigma}\boldsymbol{\varepsilon}_{ijk}L_i\left(\xi_{i'}\right)L_j\left(\eta_{j'}\right)L_k\left(\varsigma_{k'}\right), \tag{8}$$

where L_i, L_j, and L_k are the Lagrange basis functions. The introduction of Eq. (7) into Eq. (8) yields

$$\begin{aligned}\boldsymbol{\varepsilon}_{i'j'k'}&=-\sum_{i=1}^{N_\xi}\sum_{j=1}^{N_\eta}\sum_{k=1}^{N_\varsigma}\boldsymbol{B}_{ijk}L_i\left(\xi_{i'}\right)L_j\left(\eta_{j'}\right)L_k\left(\varsigma_{k'}\right)\boldsymbol{d}^{\mathrm{e}}\\ &=-\boldsymbol{B}'_{i'j'k'}\boldsymbol{d}^{\mathrm{e}},\\ \boldsymbol{B}'_{i'j'k'}&=\sum_{i=1}^{N_\xi}\sum_{j=1}^{N_\eta}\sum_{k=1}^{N_\varsigma}\boldsymbol{B}_{ijk}L_i\left(\xi_{i'}\right)L_j\left(\eta_{j'}\right)L_k\left(\varsigma_{k'}\right),\end{aligned} \tag{9}$$

where $\boldsymbol{B}'_{i'j'k'}$ is the interpolation strain matrix. Introducing the connectivity matrices of $\boldsymbol{D}_{ij}^{F}$ and $\boldsymbol{G}_{i'j'k'}$ so that $\delta\boldsymbol{u}_{ij}^{\mathrm{T}}=\delta\boldsymbol{d}^{\mathrm{eT}}\boldsymbol{D}_{ij}^{F}$ and $p_{i'j'k'}=\boldsymbol{p}^{\mathrm{eT}}\boldsymbol{G}_{i'j'k'}$, where $\boldsymbol{p}^{\mathrm{e}}$ is the element vector of pore pressure, the equilibrium equation can then be written as

$$\begin{aligned}&\boldsymbol{K}_{\mathrm{s}}^{\mathrm{e}}\boldsymbol{d}^{\mathrm{e}}+\boldsymbol{K}_{\mathrm{c}}^{\mathrm{e}}\boldsymbol{p}^{\mathrm{e}}=\boldsymbol{R}_{F}^{\mathrm{e}},\\ &\boldsymbol{K}_{\mathrm{s}}^{\mathrm{e}}=\sum_{i=1}^{N_\xi}\sum_{j=1}^{N_\eta}\sum_{k=1}^{N_\varsigma}W_iW_jW_k\boldsymbol{B}_{ijk}^{\mathrm{T}}\boldsymbol{E}_{ijk}\boldsymbol{B}_{ijk}\left|\boldsymbol{J}\right|_{ijk},\\ &\boldsymbol{K}_{\mathrm{c}}^{\mathrm{e}}=-\sum_{i'=1}^{N'_\xi}\sum_{j'=1}^{N'_\eta}\sum_{k'=1}^{N'_\varsigma}W_{i'}W_{j'}W_{k'}\boldsymbol{B}'^{\mathrm{T}}_{i'j'k'}\boldsymbol{M}\boldsymbol{G}^{\mathrm{T}}_{i'j'k'}\left|\boldsymbol{J}\right|_{i'j'k'},\\ &\boldsymbol{R}_{F}^{\mathrm{e}}=\sum_{k=1}^{N_S}\sum_{i=1}^{N_{k1}}\sum_{j=1}^{N_{k2}}W_iW_j\boldsymbol{D}_{ij}^{F}\boldsymbol{T}_{ij}\left|\bar{\boldsymbol{J}}\right|_{ij},\end{aligned} \tag{10}$$

where $\boldsymbol{K}_{\mathrm{s}}^{\mathrm{e}}$ is the stiffness matrix, $\boldsymbol{K}_{\mathrm{c}}^{\mathrm{e}}$ is the coupling matrix, and $\boldsymbol{R}_{F}^{\mathrm{e}}$ is the loading vector corresponding to the surface loads.

Similarly, the continuity equation can be numerically integrated as

$$\sum_{i'=1}^{N'_\xi}\sum_{j'=1}^{N'_\eta}\sum_{k'=1}^{N'_\varsigma} W_{i'}W_{j'}W_{k'}\left(\nabla\delta p\right)^{\mathrm{T}}_{i'j'k'}\frac{\boldsymbol{K}_{i'j'k'}}{\gamma_{\mathrm{w}i'j'k'}}\nabla p_{i'j'k'}\left|\boldsymbol{J}\right|_{i'j'k'} - \sum_{i=1}^{N_\xi}\sum_{j=1}^{N_\eta}\sum_{k=1}^{N_\varsigma} W_iW_jW_k\delta p_{ijk}\boldsymbol{M}^{\mathrm{T}}\dot{\boldsymbol{\varepsilon}}_{ijk}\left|\boldsymbol{J}\right|_{ijk} + \sum_{k'=1}^{N'_v}\sum_{i'=1}^{N'_{k1}}\sum_{j'=1}^{N'_{k2}} W_{i'}W_{j'}\delta p_{i'j'}v_{ni'j'}\left|\overline{\boldsymbol{J}}\right|_{i'j'} = 0, \tag{11}$$

where N_v' is the number of prescribed normal velocities. Then the differential quadrature analogue is introduced and the gradient of the pore pressure is

$$\begin{aligned}\nabla p_{i'j'k'} &= \begin{Bmatrix}\dfrac{\partial p}{\partial x}\\ \dfrac{\partial p}{\partial y}\\ \dfrac{\partial p}{\partial z}\end{Bmatrix}_{i'j'k'} = \boldsymbol{J}^{-1}_{i'j'k'}\begin{Bmatrix}\dfrac{\partial p}{\partial \xi}\\ \dfrac{\partial p}{\partial \eta}\\ \dfrac{\partial p}{\partial \varsigma}\end{Bmatrix}_{i'j'k'}\\ &= \boldsymbol{J}^{-1}_{i'j'k'}\begin{Bmatrix}\sum\limits_{m'=1}^{N'_\xi} C^{\xi}_{i'm'}p_{m'j'k'}\\ \sum\limits_{m'=1}^{N'_\eta} C^{\eta}_{j'm'}p_{i'm'k'}\\ \sum\limits_{m'=1}^{N'_\varsigma} C^{\varsigma}_{k'm'}p_{i'j'm'}\end{Bmatrix} = \boldsymbol{Z}^{\mathrm{T}}_{i'j'k'}\boldsymbol{p}^{\mathrm{e}},\end{aligned} \tag{12}$$

where $\boldsymbol{Z}_{i'j'k'}$ is the gradient matrix of the pore pressure. The pore pressure on some displacement node is interpolated by the pore pressures on pressure nodes:

$$\begin{aligned}p_{ijk} &= \sum_{i'=1}^{N'_\xi}\sum_{j'=1}^{N'_\eta}\sum_{k'=1}^{N'_\varsigma} p_{i'j'k'}L_{i'}\left(\xi_i\right)L_{j'}\left(\eta_j\right)L_{k'}\left(\varsigma_k\right)\\ &= \boldsymbol{p}^{\mathrm{e}\mathrm{T}}\boldsymbol{G}'_{ijk}.\end{aligned} \tag{13}$$

Introducing the connectivity matrix of $\boldsymbol{D}^{v}_{i'j'}$ so that $\delta p_{i'j'} = \delta\boldsymbol{p}^{\mathrm{e}\mathrm{T}}\boldsymbol{D}^{v}_{i'j'}$, the combination of Eqs. (11)–(13) gives

$$\begin{aligned}&\boldsymbol{K}^{\mathrm{e}}_{\mathrm{ct}}\dot{\boldsymbol{d}}^{\mathrm{e}} - \boldsymbol{K}^{\mathrm{e}}_{\mathrm{L}}\boldsymbol{p}^{\mathrm{e}} = \boldsymbol{R}^{\mathrm{e}}_{v},\\ &\boldsymbol{K}^{\mathrm{e}}_{\mathrm{ct}} = -\sum_{i=1}^{N_\xi}\sum_{j=1}^{N_\eta}\sum_{k=1}^{N_\varsigma} W_iW_jW_k\boldsymbol{G}'_{ijk}\boldsymbol{M}^{\mathrm{T}}\boldsymbol{B}_{ijk}\left|\boldsymbol{J}\right|_{ijk},\\ &\boldsymbol{K}^{\mathrm{e}}_{\mathrm{L}} = \sum_{i'=1}^{N'_\xi}\sum_{j'=1}^{N'_\eta}\sum_{k'=1}^{N'_\varsigma}\frac{1}{\gamma_{\mathrm{w}i'j'k'}}W_{i'}W_{j'}W_{k'}\boldsymbol{Z}_{i'j'k'}\boldsymbol{K}_{i'j'k'}\boldsymbol{Z}^{\mathrm{T}}_{i'j'k'}\left|\boldsymbol{J}\right|_{i'j'k'},\\ &\boldsymbol{R}^{\mathrm{e}}_{v} = \sum_{k'=1}^{N'_v}\sum_{i'=1}^{N'_{k1}}\sum_{j'=1}^{N'_{k2}} W_{i'}W_{j'}\boldsymbol{D}^{v}_{i'j'}v_{ni'j'}\left|\overline{\boldsymbol{J}}\right|_{i'j'},\end{aligned} \tag{14}$$

where $\boldsymbol{K}^{\mathrm{e}}_{\mathrm{ct}}$ is the coupling matrix, $\boldsymbol{K}^{\mathrm{e}}_{\mathrm{L}}$ is the element permeability matrix, and $\boldsymbol{R}^{\mathrm{e}}_{v}$ is the loading vector corresponding to the prescribed normal velocity. The two-point marching scheme is used for time integration:

$$\begin{aligned}\int_{t_n}^{t_{n+1}} f\left(t\right)\mathrm{d}t &= \left(1-\theta\right)f\left(t_n\right)\Delta t + \theta f\left(t_{n+1}\right)\Delta t,\\ \Delta t &= t_{n+1} - t_n,\end{aligned} \tag{15}$$

where t_n and t_{n+1} denote the respective time at the nth and (n+1)th steps, and θ is a weighting parameter. θ=0 indicates forward interpolation, θ=0.5 represents the Crank-Nicolson method, θ=2/3 corresponds to the Galerkin method, and θ=1 indicates backward Euler interpolation, which will be employed in the following examples unless noted otherwise. Applying Eq. (15) into Eqs. (10) and (14), we obtain the final algebraic equations as

$$\begin{aligned}&\begin{Bmatrix}\boldsymbol{K}^{\mathrm{e}}_{\mathrm{s}} & \boldsymbol{K}^{\mathrm{e}}_{\mathrm{c}}\\ \boldsymbol{K}^{\mathrm{e}}_{\mathrm{ct}} & -\theta\Delta t\boldsymbol{K}^{\mathrm{e}}_{\mathrm{L}}\end{Bmatrix}\begin{Bmatrix}\Delta\boldsymbol{d}^{\mathrm{e}}\\ \Delta\boldsymbol{p}^{\mathrm{e}}\end{Bmatrix} = \begin{Bmatrix}\Delta\boldsymbol{R}^{\mathrm{e}}_{F}\\ \Delta\boldsymbol{R}^{\mathrm{e}}_{p}\end{Bmatrix},\\ &\Delta\boldsymbol{R}^{\mathrm{e}}_{p} = \Delta t\left(\boldsymbol{R}^{\mathrm{e}}_{v} + \boldsymbol{K}^{\mathrm{e}}_{\mathrm{L}}\boldsymbol{p}^{\mathrm{e}}_{n}\right),\\ &\boldsymbol{d}^{\mathrm{e}}_{n+1} = \boldsymbol{d}^{\mathrm{e}}_{n} + \Delta\boldsymbol{d}^{\mathrm{e}},\\ &\boldsymbol{p}^{\mathrm{e}}_{n+1} = \boldsymbol{p}^{\mathrm{e}}_{n} + \Delta\boldsymbol{p}^{\mathrm{e}},\end{aligned} \tag{16}$$

where the subscript n denotes the number of time increments. After the assemblage of Eq. (16) for every element in the global system, the coupled consolidation behavior of soils can be modeled progressively with given initial and boundary conditions.

Note that if the integration of the pore water pressure and the pore air pressure is taken as one order higher than that of the displacement, the composite element for unsaturated consolidation can be established using the same procedure. On the other hand, it is well known that soil creep occurs concurrently with consolidation after external loading. To describe creep behavior accurately, it is necessary to develop

realistic creep models and appropriate ways for determining the corresponding parameters. Recently, some developments have been made regarding the determination of creep parameters using optimization procedures (Le and Fatahi, 2016; Le et al., 2016). However, the scope of the present study was confined to saturated soils, and for conciseness soil, creep was not considered.

4 Numerical examples

In the following examples, quadrilateral quadrature elements are used for 1D and 2D consolidation problems. Note that if equal order integration is used for the displacement and the pore pressure, i.e.

$$N'_{\xi}=N_{\xi},\quad N'_{\eta}=N_{\eta},\quad N'_{\varsigma}=N_{\varsigma}, \tag{17}$$

the formulations derived above turn into those of the standard element.

4.1 One-dimensional consolidation

The 1D problem shown in Fig. 2 was analyzed using the proposed element. For convenience, some non-dimensional quantities are introduced:

$$\underline{x}=\frac{x}{H},\quad \underline{t}=\frac{\left(\hat{\lambda}+2\hat{\mu}\right)k_{\mathrm{w}}t}{\gamma_{\mathrm{w}}H^{2}},\quad \underline{p}=\frac{p}{p_{0}}, \tag{18}$$

where $\hat{\lambda}$ and $\hat{\mu}$ are the Lamé coefficients, t is the time, k_{w} is the permeability, and the definitions of other parameters are shown in Fig. 2. The analytical solution for this specific case is

$$\underline{p}_{\mathrm{exa}}\left(\underline{x},\underline{t}\right)=\sum_{i=0}^{\infty}\frac{2}{N}\sin\left(N\underline{x}\right)\exp\left(-N^{2}\underline{t}\right),\quad N=\frac{\pi\left(2i+1\right)}{2}. \tag{19}$$

One standard element with 15 nodes and one composite element with 15 pressure nodes were employed and the non-dimensional time increment was taken as 10^{-5}, 10^{-6}, and 10^{-7} to study the effect of the time increment. The pore pressures obtained at $\underline{t}=10^{-5}$ are given in Fig. 3. Obviously, oscillations caused by the standard element of the QEM were significant, but were greatly reduced by the composite element. The influence of the time increment was not significant for the case considered. Moreover, the time increment had less impact on the results of the composite element than on the results of the standard element. The results obtained by multiple elements using the time increment of 10^{-6} are shown in Fig. 4, where five standard elements and five composite elements with seven pressure nodes in each element were used and the stabilization effect was reflected once again.

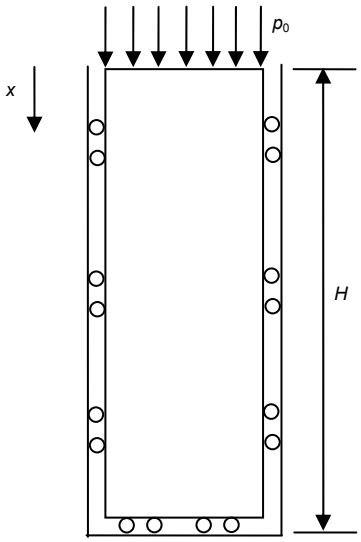


Fig. 2 One-dimensional consolidation

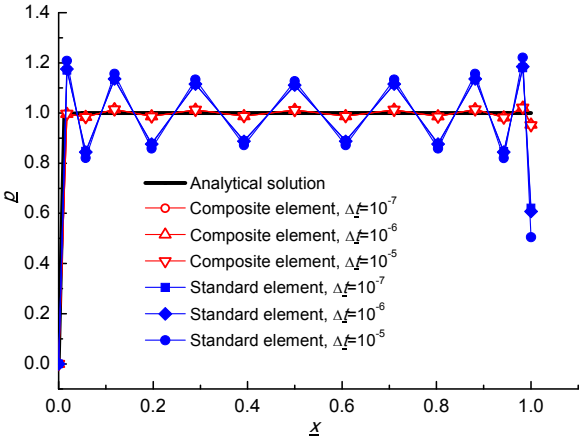


Fig. 3 Pore pressures obtained using one quadrature element

As concluded by Sandhu et al. (1977), low accuracy of the initial settlement would be achieved if a

composite element was used. This will be investigated in the framework of the QEM. The settlement was calculated by one standard element and one composite element. To make sure the comparison was made under the same conditions, 15 displacement nodes were used in each of the two kinds of element, which means that the approximation of pore pressure of the composite element was one order lower than that of the standard element. The settlement and the relative errors are given in Fig. 5, where $\underline{u}$ and $\underline{u}_{\mathrm{exa}}$ denote the non-dimensional vertical displacement and the corresponding analytical solution, respectively. Note that in the initial stage of consolidation, i.e. $\underline{t}<10^{-3}$, the accuracy of the composite element was low compared with that of the standard element, but the accuracy of the two elements was otherwise similar.

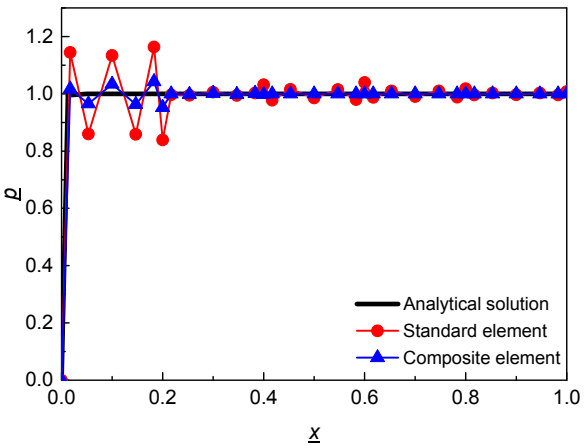


Fig. 4 Pore pressures obtained using five quadrature elements

It is well known that second-order accuracy can be reached if the Crank-Nicolson scheme is used for time integration. Nevertheless, the pressure oscillations discussed above will not disappear with time and another type of oscillation will arise at some point in the time evolution curve of the pore pressure. The Crank-Nicolson scheme was adopted and examined in the QEM. Fifteen pressure nodes were chosen for the standard and composite elements and the time increments were taken as $\Delta\underline{t}_{n+1}=1.4\Delta\underline{t}_n$, $\Delta\underline{t}_1=10^{-4}$. The time history of the pore pressure at $\underline{x}=0.1969$ is given in Fig. 6. Note that oscillations produced in the evolution curve of pore pressure when the Crank-Nicolson scheme is applied could be eliminated by the use of the composite element, which also improved accuracy to a large extent.

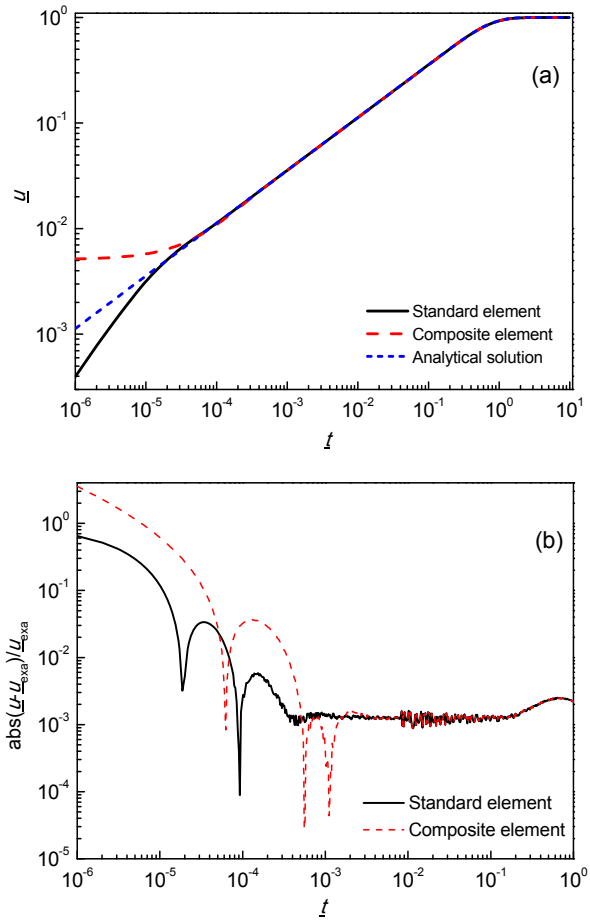


Fig. 5 Evolution (a) and the relative errors (b) of the settlement

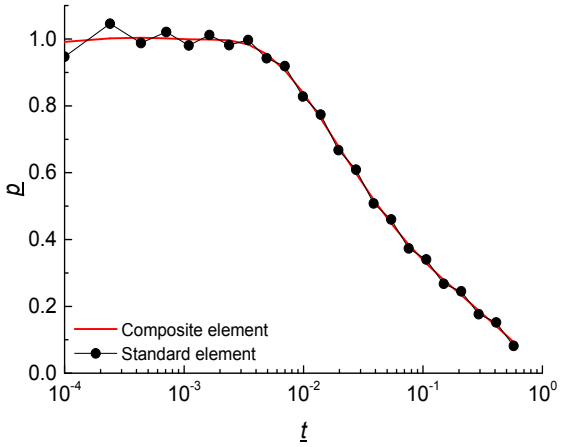


Fig. 6 Time history of the pore pressure at $\underline{x}=0.1969$

The soil column was then assumed to be subjected to a fixed pumping rate of 10^{-6} m/s at the top surface. The parameters for the problem were respectively taken as H=10 m, $\hat{\lambda}$ =5.77 MPa, $\hat{\mu}$ = 3.85 MPa, k_w=10^{-4} m/s, and Δt=0.001 d. Pore pressure profiles at different times are given in Fig. 7, where the reference values were obtained by the standard quadrature elements with 45 integration points. It can be clearly seen that the proposed element also performed very well for problems with given flux boundary conditions. On the other hand, the results were in close agreement when the pore pressure became smooth.

4.2 Two-dimensional consolidation

In this example, a 2D problem was studied (Fig. 8). A foundation was suddenly loaded by a uniform pressure p_0. The material properties of the foundation were: k_w=10^{-3} m/s, $\hat{\lambda}$ =0, $\hat{\mu}$ =5 MPa, and the time increment is taken as 10^{-6} s. Four elements were meshed with 8×8 pressure nodes in each standard and composite element. The pore pressures along the centerline of the foundation at 10^{-5} s are shown in Fig. 9, and the contours of the pore pressure at 10^{-5} s obtained by standard elements and composite elements are given in Fig. 10. It can be seen that the pore pressure was stabilized effectively by the proposed element for the 2D consolidation problem.

4.3 Consolidation of a cylinder

In this example, the consolidation of a cylinder internally loaded by a uniform pressure of 100 kPa was analyzed (Fig. 11). The internal radius R_1 was taken as 0.1 m, 0.25 m, 0.5 m, and 1 m and the external radius R_2 was 2 m, with all the material properties described in Section 4.2. It was pervious at the internal surface and impervious at the external surface. For the symmetry of the problem, one fourth of the cylinder was considered. One standard and one composite quadrature elements were employed with

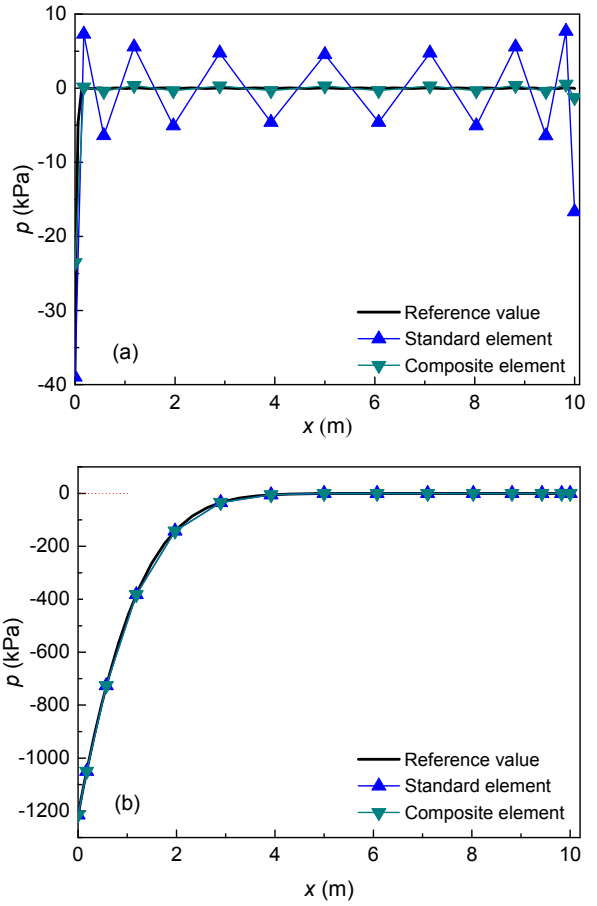


Fig. 7 Pore pressures of the example with given flux boundary conditions: (a) t=0.01 d; (b) t=1 d

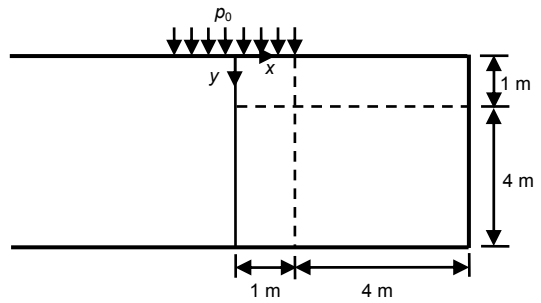


Fig. 8 Two-dimensional consolidation

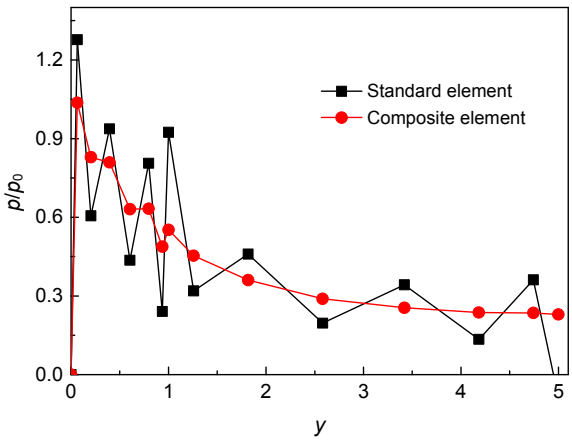


Fig. 9 Pore pressures along the center line of the foundation

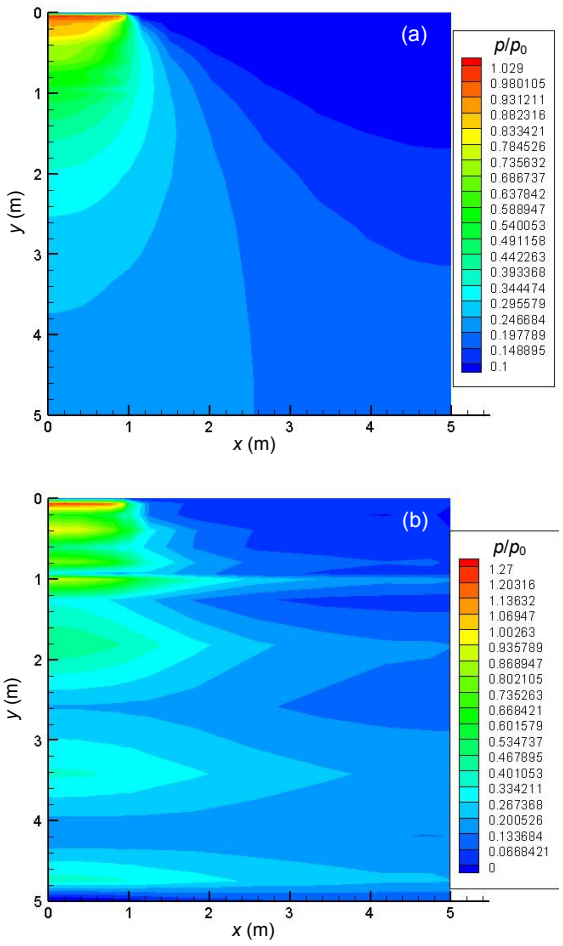


Fig. 10 Pore pressure contours of the foundation obtained using composite elements (a) and standard elements (b)

15×15 integration points. To describe the cylinder more precisely, the blending functions were adopted to transform the cylinder into the normalized domain, which can be expressed as

$$\begin{aligned}\theta&=\frac{1-\eta}{2}\times 0+\frac{1+\eta}{2}\times\frac{\pi}{2}=\frac{(1+\eta)\pi}{4},\\ R&=\frac{1-\xi}{2}R_1+\frac{1+\xi}{2}R_2,\\ x&=R\cos\theta=\left(\frac{1-\xi}{2}R_1+\frac{1+\xi}{2}R_2\right)\cos\left(\frac{(1+\eta)\pi}{4}\right),\\ y&=R\sin\theta=\left(\frac{1-\xi}{2}R_1+\frac{1+\xi}{2}R_2\right)\sin\left(\frac{(1+\eta)\pi}{4}\right),\end{aligned}\tag{20}$$

where R and θ are the polar coordinates as shown in Fig. 11. The contours of the pore pressure at 10^{-5} s are shown in Figs. 12 and 13, which show that stabilized results can be obtained for all cases considered. With the decrease of the internal radius, the oscillations produced by the standard elements tended to concentrate around the cavity. However, this had little effect on the numerical performance of the composite elements.

4.4 Undrained triaxial test

An undrained saturated triaxial test was simulated in this example. To evaluate the performance of the proposed element for elasto-plastic consolidation analysis, the bounding surface model (Manzari and Dafalias, 1997; Fei and Liu, 2009) is introduced. Five material parameters are required: Poisson's ratio μ_0, the slope of the critical state line (CSL) M, the slope of the normal consolidation line (NCL) λ, the slope of the unloading-rebound line (URL) κ, and a model constant H_0, which were respectively taken as 0.3, 1.1, 0.017, 0.034, and 20. The pre-consolidation pressure was 300 kPa and the initial mean effective stress σ_m' was taken as 300 kPa or 75 kPa to give an over consolidation ratio (OCR) of 1 or 4, respectively.

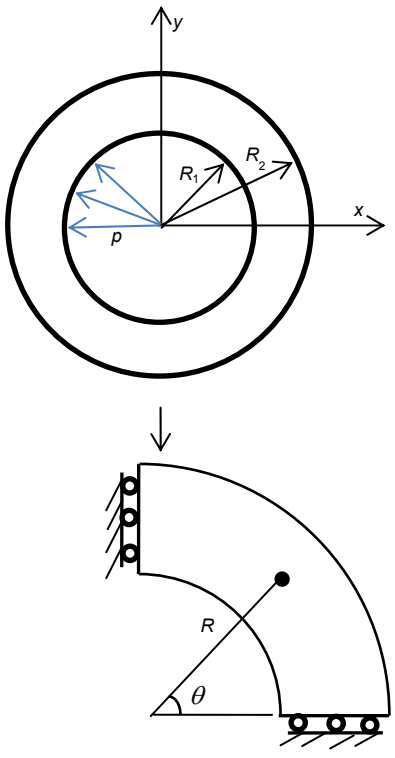


Fig. 11 Internally pressurized cylinder

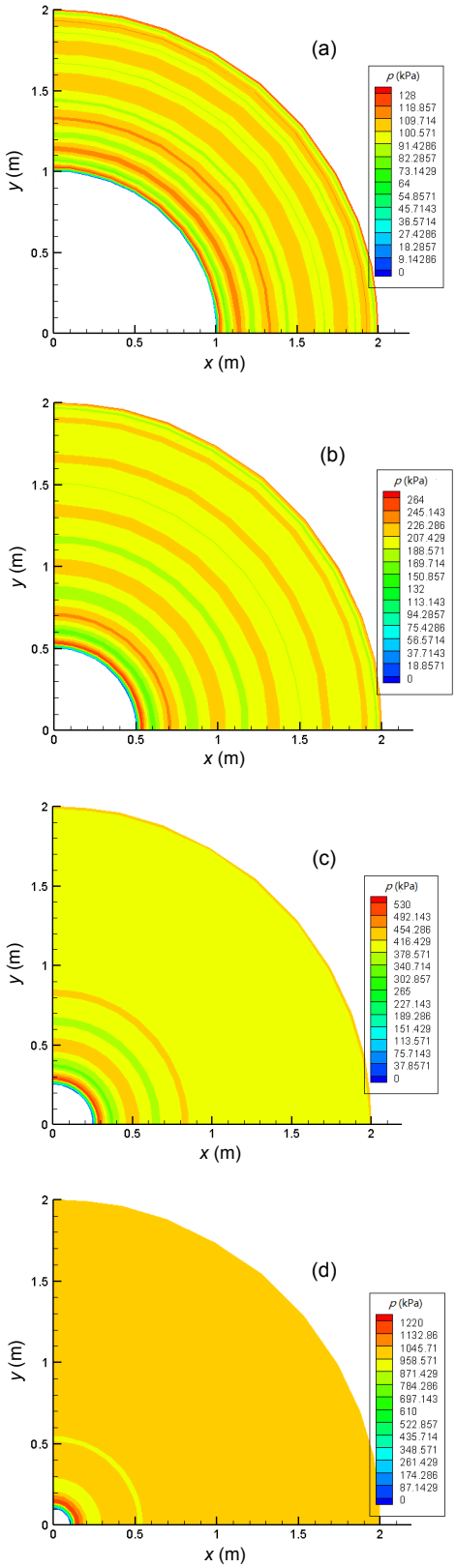


Fig. 12 Pore pressures of the cylinder obtained using standard elements
(a) R_1=1 m; (b) R_1=0.5 m; (c) R_1=0.25 m; (d) R_1=0.1 m

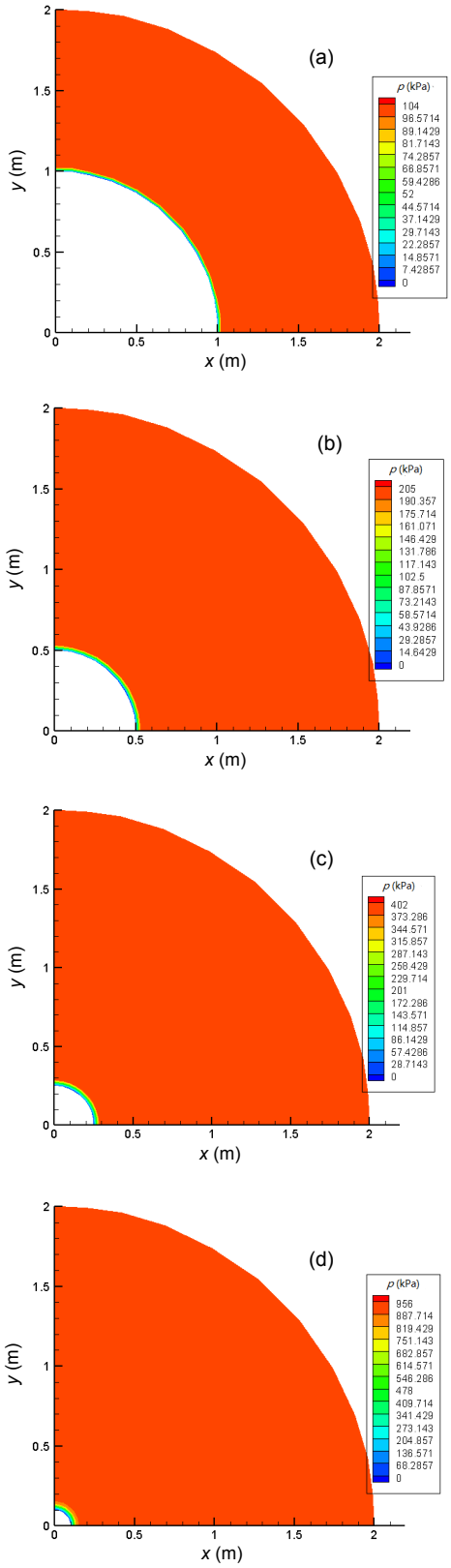


Fig. 13 Pore pressures of the cylinder obtained using composite elements
(a) R_1=1 m; (b) R_1=0.5 m; (c) R_1=0.25 m; (d) R_1=0.1 m

Both the standard and composite elements were used. The stress paths obtained and the variation of the pore pressures are given in Fig. 14, where $q=\sigma_1-\sigma_3$ is the deviatoric stress and ε_a is the axial strain. It can be seen that positive pore pressures were generated during the test for normal consolidated soils, whereas negative pressures were induced for over consolidated soils. As a result, the stresses of normal and over consolidated soils reached CSL from the wet and dry sides, respectively. The deviatoric stress of over consolidated soils reached a peak value and subsequently decreased to the corresponding maximum value of normal consolidated soils. The results confirm that typical mechanical behaviors of normal consolidated and over consolidated soils can be represented effectively and the performance of the two elements is similar when the distribution of the pore pressure is smooth.

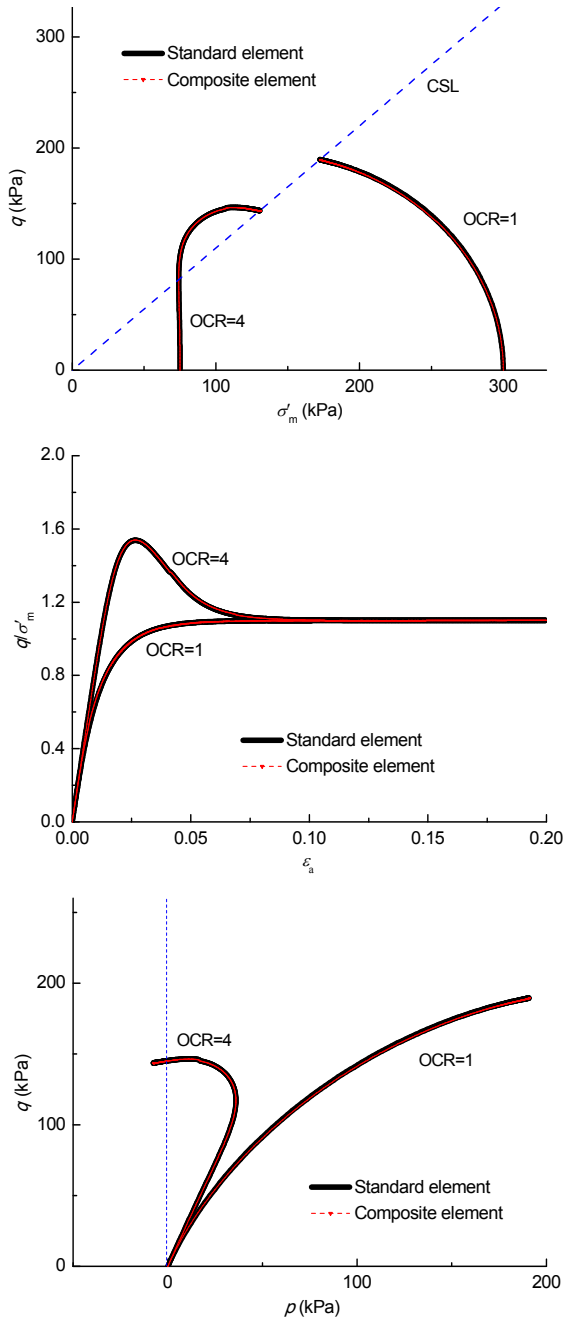


Fig. 14 Stress paths and variation in the pore pressure in the undrained triaxial test

5 Conclusions

A composite quadrature element is proposed for consolidation analysis to overcome the oscillations produced when small time increments are chosen. The element involves integration of the displacement one order higher than that of the pore pressure. Different nodes are employed for the displacement and the pore pressure, except those on the corner of the element. Strains at the pressure nodes and pore pressures at the displacement nodes are approximated through Lagrange interpolation. Performance of the composite element was investigated and compared with that of the standard element through numerical tests of 1D and 2D consolidation. The results show that oscillations generated when small time steps are used and those induced by the Crank-Nicolson scheme are greatly reduced by the proposed element, and the accuracy is also greatly improved.

References

Aguilar G, Gaspar F, Lisbona F, et al., 2008. Numerical stabilization of Biot's consolidation model by a perturbation on the flow equation. *International Journal for Numerical Methods in Engineering*, 75(11):1282-1300. https://doi.org/10.1002/nme.2295

Azari B, Fatahi B, Khabbaz H, 2015. Numerical analysis of vertical drains accelerated consolidation considering combined soil disturbance and visco-plastic behaviour. *Geomechanics & Engineering*, 8(2):187-220. https://doi.org/10.12989/gae.2015.8.2.187

Bellman R, Casti J, 1971. Differential quadrature and long-term integration. *Journal of Mathematical Analysis and Applications*, 34(2):235-238. https://doi.org/10.1016/0022-247X(71)90110-7

Biot MA, 1941. General theory of three-dimensional consolidation. *Journal of Applied Physics*, 12(2):155-164. https://doi.org/10.1063/1.1712886

Boal N, Gaspar FJ, Lisbona FJ, et al., 2011. Finite-difference analysis of fully dynamic problems for saturated porous media. *Journal of Computational and Applied Mathematics*, 236(6):1090-1102. https://doi.org/10.1016/j.cam.2011.07.032

Chen R, Zhou W, Wang H, et al., 2005. One-dimensional nonlinear consolidation of multi-layered soil by differential quadrature method. *Computers and Geotechnics*, 32(5):358-369. https://doi.org/10.1016/j.compgeo.2005.05.003

Darkshanamurthy V, Fredlund DG, Rahardjo H, 1984. Coupled three-dimensional consolidation theory of unsaturated porous media. Fifth International Conference on Expansive Soils, p.99.

Fei K, Liu HL, 2009. Implementation and application of bounding surface model in ABAQUS. *Journal of PLA University of Science and Technology (Natural Science Edition)*, 10(5):447-451 (in Chinese).

Gaspar FJ, Lisbona FJ, Vabishchevich PN, 2003. A finite difference analysis of Biot's consolidation model. *Applied Numerical Mathematics*, 44(4):487-506. https://doi.org/10.1016/S0168-9274(02)00190-3

Gaspar FJ, Lisbona FJ, Vabishchevich PN, 2006. Staggered grid discretizations for the quasi-static Biot's consolidation problem. *Applied Numerical Mathematics*, 56(6): 888-898. https://doi.org/10.1016/j.apnum.2005.07.002

Gaspar FJ, Lisbona FJ, Matus P, et al., 2016. Numerical methods for a one-dimensional non-linear Biot's model. *Journal of Computational and Applied Mathematics*, 293: 62-72. https://doi.org/10.1016/j.cam.2015.03.039

Ho L, Fatahi B, 2015. Analytical solution for the two-dimensional plane strain consolidation of an unsaturated soil stratum subjected to time-dependent loading. *Computers & Geotechnics*, 67:1-16. https://doi.org/10.1016/j.compgeo.2015.02.011

Ho L, Fatahi B, Khabbaz H, 2016. Analytical solution to axisymmetric consolidation in unsaturated soils with linearly depth-dependent initial conditions. *Computers & Geotechnics*, 74:102-121. https://doi.org/10.1016/j.compgeo.2015.12.019

Hua L, 2011. Stable element—free Galerkin solution procedures for the coupled soil—pore fluid problem. *International Journal for Numerical Methods in Engineering*, 86(8):1000-1026. https://doi.org/10.1002/nme.3087

Le TM, Fatahi B, 2016. Trust-region reflective optimisation to obtain soil visco-plastic properties. *Engineering Computations*, 33(2):410-442. https://doi.org/10.1108/EC-11-2014-0236

Le TM, Fatahi B, Khabbaz H, et al., 2016. Numerical optimisation applying trust-region reflective least squares algorithm with constraints to optimise the non-linear creep parameters of soft soil. *Applied Mathematical Modelling*, 16:1-21.

Manzari MT, Dafalias YF, 1997. A critical state two-surface plasticity model for sands. *Geotechnique*, 47(2):255-272. https://doi.org/10.1680/geot.1997.47.2.255

Mira P, Pastor M, Li T, et al., 2003. A new stabilized enhanced strain element with equal order of interpolation for soil consolidation problems. *Computer Methods in Applied Mechanics and Engineering*, 192(37-38):4257-4277. https://doi.org/10.1016/S0045-7825(03)00416-X

Preisig M, Prévost JH, 2011. Stabilization procedures in coupled poromechanics problems: a critical assessment. *International Journal for Numerical and Analytical Methods in Geomechanics*, 35(11):1207-1225. https://doi.org/10.1002/nag.951

Reed M, 1984. An investigation of numerical errors in the analysis of consolidation by finite elements. *International Journal for Numerical and Analytical Methods in Geomechanics*, 8(3):243-257. https://doi.org/10.1002/nag.1610080304

Rodrigo C, Gaspar F, Hu X, et al., 2016. Stability and monotonicity for some discretizations of the Biot's consolidation model. *Computer Methods in Applied Mechanics and Engineering*, 298:183-204. https://doi.org/10.1016/j.cma.2015.09.019

Samimi S, Pak A, 2012. Three-dimensional simulation of fully coupled hydro-mechanical behavior of saturated porous media using element free Galerkin (EFG) method. *Computers & Geotechnics*, 46(4):75-83. https://doi.org/10.1016/j.compgeo.2012.06.004

Sandhu RS, Liu H, Singh KJ, 1977. Numerical performance of some finite element schemes for analysis of seepage in porous elastic media. *International Journal for Numerical and Analytical Methods in Geomechanics*, 1(2):177-194. https://doi.org/10.1002/nag.1610010205

Simo JC, Rifai M, 1990. A class of mixed assumed strain methods and the method of incompatible modes. *International Journal for Numerical Methods in Engineering*, 29(8):1595-1638. https://doi.org/10.1002/nme.1620290802

Wang W, Wang J, Wang Z, et al., 2007. An unequal-order radial interpolation meshless method for Biot's consolidation theory. *Computers and Geotechnics*, 34(2):61-70. https://doi.org/10.1016/j.compgeo.2006.10.010

Wang X, Gu H, 1997. Static analysis of frame structures by the differential quadrature element method. *International Journal for Numerical Methods in Engineering*, 40(4): 759-772. https://doi.org/10.1002/(SICI)1097-0207(19970228)40:4<759::AID-NME87>3.0.CO;2-9

Yuan S, Zhong HZ, 2014. Consolidation analysis of non-homogeneous soil by the weak form quadrature element method. *Computers and Geotechnics*, 62:1-10. https://doi.org/10.1016/j.compgeo.2014.06.012

Yuan S, Zhong HZ, 2016a. Three dimensional analysis of unconfined seepage in earth dams by the weak form quadrature element method. *Journal of Hydrology*,

533:403- 411.
https://doi.org/10.1016/j.jhydrol.2015.12.034

Yuan S, Zhong HZ, 2016b. A weak form quadrature element formulation for coupled analysis of unsaturated soils. *Computers and Geotechnics*, 76:1-11.
https://doi.org/10.1016/j.compgeo.2016.02.006

Yuan S, Zhong HZ, 2017. Finite deformation elasto-plastic consolidation analysis of soft clay by the weak form quadrature element method. *Journal of Zhejiang University-SCIENCE A (Applied Physics & Engineering)*, 18(12):942-957.
https://doi.org/10.1631/jzus.A1600671

Zhong HZ, Yu T, 2009. A weak form quadrature element method for plane elasticity problems. *Applied Mathematical Modelling*, 33(10):3801-3814.
https://doi.org/10.1016/j.apm.2008.12.007

中文概要

题　目： 一种非等阶积分的求积元孔压单元

目　的： 在对土体固结问题进行求解时，如果对孔压和位移采用等阶积分，当时间步长取值很小时，得到的孔压结果会出现数值振荡，导致精度降低。本文提出一种非等阶积分的求积元孔压单元，致力于减小孔压振荡，提高单元稳定性和计算精度。

创新点： 1. 建立了一种对于孔压和位移采用不同阶积分的求积元复合单元；2. 有效降低了小时间步长引起的孔压振荡。

方　法： 1. 通过求积元法对弱形式控制方程进行数值积分，并对比奥固结方程中的位移项和孔压项采用不等阶积分；2. 通过拉格朗日插值获得位移点上的孔压和孔压点上的位移值；3. 通过一维及二维问题的数值算例，验证所建立方法的有效性。

结　论： 1. 通过采用复合求积元单元，大大降低了孔压的数值振荡；2. 应用复合求积单元时，采用二阶精度的 Crank-Nicolson 积分格式不会产生随时间的孔压振荡；3. 本文所建立的单元可以大大提高固结问题求解的数值计算精度和计算效率。

关键词： 弱形式求积元法；不等阶积分；孔压振荡；固结分析